HAL
open science

Optimising punctual water sampling with an on-the-fly algorithm based on multiparameter high-frequency measurements

Jérémy Mougin, Pierre-Jean Superville, Cyril Ruckebusch, Gabriel Billon

To cite this version:

Jérémy Mougin, Pierre-Jean Superville, Cyril Ruckebusch, Gabriel Billon. Optimising punctual water sampling with an on-the-fly algorithm based on multiparameter high-frequency measurements. Water Research, 2022, 221, pp.118750. 10.1016/j.watres.2022.118750 . hal-03715742

HAL Id: hal-03715742

https://hal.science/hal-03715742

Submitted on 5 Feb 2024

HAL is a multi-disciplinary open access archive for the deposit and dissemination of scientific research documents, whether they are published or not. The documents may come from teaching and research institutions in France or abroad, or from public or private research centers.

L'archive ouverte pluridisciplinaire **HAL**, est destinée au dépôt et à la diffusion de documents scientifiques de niveau recherche, publiés ou non, émanant des établissements d'enseignement et de recherche français ou étrangers, des laboratoires publics ou privés.

Optimising punctual water sampling with an on-the-fly algorithm based on multiparameter high-frequency measurements

Jérémy Mougin[1], Pierre-Jean Superville[1], Cyril Ruckebusch[1], Gabriel Billon[1]*

[1]Université Lille, CNRS, UMR 8516 - LASIRE, LAboratoire de Spectroscopie pour les Interactions, la Réactivité et l'Environnement, F-59000 Lille, France.

* corresponding author

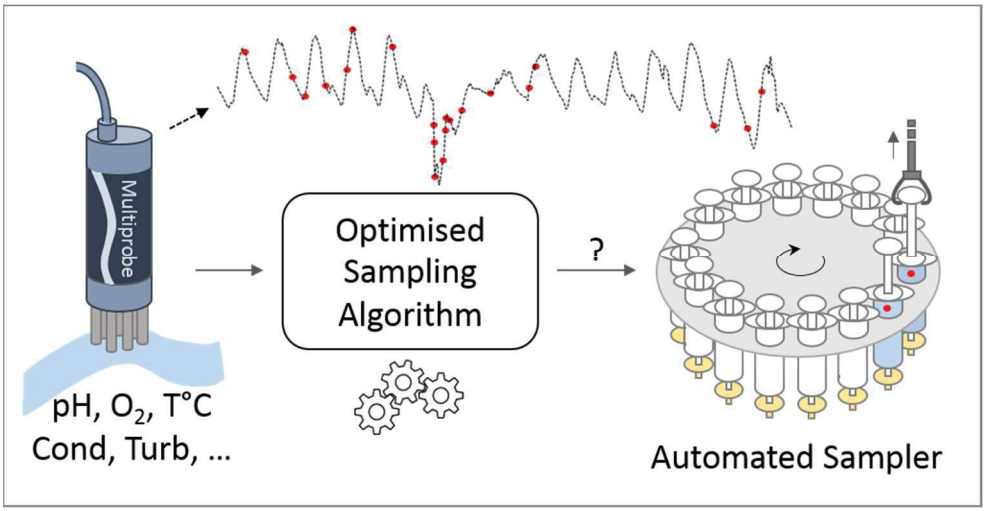

Highlights :

- Optimised sampling to replace time-consuming high frequency sampling
- On-the-fly decision algorithm based on multiparameter measurements
- Reduction of the number of samples while retaining the dataset variability
- Systematic sampling of short events with a strong impact on the environment

Abstract:

The way in which aquatic systems is sampled has a strong influence on our understanding of them, especially when they are highly dynamic. High frequency sampling has the advantage over spot sampling for representativeness but leads to a high amount of analysis. This study proposes a new methodology to choose when sampling accurately with an automated sampler coupled with a high frequency (HF) multiparameter probe. After each HF measurement, an optimised sampling algorithm (OSA) determines on-the-fly the relevance of taking a new sample in relation to previous waters already collected. Once the OSA was optimised, considering the number of HF parameters and their variabilities, it was demonstrated through a study case that the number of samples could be significantly reduced, while still covering periods of low and high variabilities. The comparison between the total HF dataset and the sampled subdataset shows that physicochemical parameter variability is preserved (Pearson correlations > 0.96) as well as the multiparameter variability (PCA axes remained similar with Tucker congruence > 0.99). This algorithm simplifies HF studies by making it easier to take samples during brief phenomena such as storms or accidental spills that are often poorly monitored. In addition, it optimises the number of samples to be taken to correctly describe a system and thus reduce the human and financial costs of these environmental studies.

Keywords: river, monitoring, on line, high frequency, algorithm, sampling

Introduction

The composition and quality of aquatic systems are well known to be highly dynamic due to physical, biological, chemical, meteorological, and climatic factors. All these pressures have an impact on the environment quality and take place on very different scales, from minutes to years, and few square meters up to full catchments (Aguilera et al. 2016; Halliday et al. 2014; Meyer et al. 2021; Rode et al. 2016). Daily cycles resulting from recurring environmental phenomena, such as photosynthesis or temperature fluctuations (Halliday et al. 2014; Nimick et al. 2011; Shultz et al. 2018; Superville et al. 2014) are the most usually observed. Quick punctual events can also be recorded such as heavy rainfalls or industrial discharges, which are hardly predictable (Khamis et al. 2020; Seifert-Dähnn et al. 2021; Vaughan et al. 2019). At a much larger time scale, seasonal effects can be critical, as for algal bloom and the resulting organic matter decomposition, which can dramatically affect water quality (Seifert et al. 2016).

Monitoring aquatic ecosystems with an inadequate measurement frequency may lead to missing information and/or misinterpretation of the observed data (Marcé et al. 2016). It is therefore necessary to implement monitoring methods adapted to the environments studied and their dynamics. To address this scientific challenge, automated HF monitoring is a growing trend for operational and research purposes (Bieroza and Heathwaite 2015; Gunatilaka and Diehl 2001; Halliday et al. 2014; Ivanovsky et al. 2016; Khamis et al. 2020; Rode et al. 2016; Seifert-Dähnn et al. 2021). The capacity to measure *in situ* or *on-line* was strongly enhanced during the last decades. Miniaturization, increased power capacity and technological advances in probes have allowed new sensors to be deployed with a better stability over time (Marcé et al. 2016). However, numerous parameters, *e.g.* micro-pollutants, cannot be easily monitored due to the lack of specific on line probe or analyser and/or intensive maintenance work requirement (Khamis et al. 2020; Marcé et al. 2016).

To overcome these limitations, most studies still rely on taking samples for off-line laboratory analysis, where a wider range of parameters can be studied. However, as the aquatic ecosystems are quickly evolving, the relevance of each sample depends strongly on when and where it was taken (Meyer et al. 2021; Piniewski et al. 2019). To be able to monitoring short-term phenomena, the increase of samples number is paramount (Khamis et al. 2020). However, some phenomena are not predictable and a strong increase in the sampling frequency (for instance several per day) is not operationally sustainable for a long term. Moreover, the probability of sampling a specific event of short duration is very low (Carstea et al. 2010) and it may lead to a misunderstanding of certain processes (Aguilera et al. 2016; Bieroza and Heathwaite 2016; Jarvie et al. 2018; Marcé et al. 2016; Reynolds et al. 2016).

For limnological studies, the number of samples needed to properly represents the environment can be relatively large (Aguilera et al. 2016). Some sampling strategies are based on a preliminary HF monitoring that allows for the optimisation of the sampling frequency (Aguilera et al. 2016; Ferrant et al. 2013; Piniewski et al. 2019). Another solution is to take only a few samples and rely on modelling tools to extrapolate the data (Searcy and Boehm 2021). However, these tools are not always well adapted and may provide information that is contradictory to the observations (Liu et al. 2018; Piniewski et al. 2019).

Our work establishes an alternative sampling solution. The main idea is to use the HF measurements data on-the-fly as a decision tool to choose when to sample next. The HF measurements are used as a visualization of the chemical status of the water body, and to trigger an automated sampler based on recorded variations. Samplers triggered by the variation of one parameter (*e.g.* conductivity or turbidity) have been previously used in environmental monitoring (Lewis and Eads 2009) but as far as we know, there are no systems based on a multivariate approach. The aims of this methodology are: (i) to minimise the number of off-line analysis without losing information from specific phenomena; and (ii) to hold data data

variability, statistical relevance and robustness of the off-line analysis. An application in the field illustrates critically the proof of concept of this innovative procedure.

1. Material & Methods

1.1. Study site

The study site is the Marque River, located in Northern France close to Lille. It has a length of 32 km, an average flow at its confluence of 1.2 $m^3 s^{-1}$ and crosses an agricultural area in its upstream part and a more urban basin downstream. It is fed mainly by runoff, as well as by 8 urban wastewater treatment plants (WWTP). WWTPs discharges can provide up to 30% of the Marque River flow during dry periods close to the study site. According to the Water Framework Directive criteria, its chemical and ecological quality is poor due to the presence of significant amounts of nitrogen, phosphorus, pesticides and Polycyclic Aromatic Hydrocarbons (HAP). The monitoring station (50°38'43.6"N, 3°10'54.5"E) is located at the beginning of the urban part, about 1 km downstream of the Villeneuve d'Ascq WWTP (144 000 Equivalent inhabitant) and 300 m downstream of the discharge of a rainwater retention basin (Heron lake, 634 000 m^3) (Ivanosky et al., 2016; Ivanovsky et al., 2018; Trommetter et al., submitted).

1.2. High frequency monitoring set up

Mobile Laboratory – On line monitoring is carried out using a mobile laboratory (ML), designed, and equipped to measure various physicochemical parameters in the field. This type of infrastructure has already been used for similar monitoring (Ivanovsky et al. 2016; Meyer et al. 2021). It is a trailer that can be towed by a commercial vehicle and can be deployed close to the water body (power supply is however necessary). It is equipped with an air conditioning system allowing to keep a relative constant temperature of 15-25°C. A submersible pump (water flow: 10~15 $m^3 h^{-1}$) supplies the ML and its various analysis devices. Briefly, most of the raw

water pumped is first introduced into an overflow cell in which a multiparameter probe is immersed. The overflow cell allows a measurement as close as possible to an *in-situ* measurement, allowing the constant renewal of the sample and an efficient transport of suspended matter. The second part of the hydraulic system includes an output to supply a homemade automatic filtering sampler and another output with an online filter at 100 µm which mainly protects nutrients analysers from the biggest suspended matter. Finally, data acquired are transmitted every 30 minutes via a 4g network to a storage server, allowing the river to be monitored remotely and the whole system (pump, probes…) to be checked regularly.

Multiprobe and automatic filtering sampler - High frequency monitoring is performed with a multiprobe (*Eureka Water Probes; Manta+35*). It allows the monitoring of 7 chemical parameters: temperature, pH, conductivity, turbidity, dissolved oxygen and two fluorescence probes (*Turner Design*) for the measurement of DOM (1 sensitive to coloured dissolved organic matter (CDOM) and 1 sensitive to tryptophan-like substances). Every 10 minutes, a python script communicates with this probe, activates a wiper to clean the optical probes, and collects the average values of 10 sucessive measurements for each parameter (*Python Software Foundation*. Python Language Reference, version 3.7.). After each measurement, a decision algorithm (see section *sampling methodology*) analyses the new values and decides whether to trigger a sampling. If it is the case, a signal is sent to an automatic filtering sampler equipped with a 0.7 µm filter (glass microfiber, Whatman) to eliminate most of the suspended matter. This homemade instrument consists of a carousel on which 24 syringes are placed and operating with a mechanical jack. As the samples are not refrigerated in the sampler, they are recovered as soon as possible (maximum 3 days) and then kept at 4°C before analyses in the laboratory (within the week).

1.3. Sampling methodology

Overview - The sample selection strategy developed in this work consists in collecting a sample on "each state" of the aquatic system that can be observed by the multi-probe. A state is defined as a combination of the values of the 7 parameters measured by the probe (± a certain margin). By capturing only discrete samples, the main objective of this methodology is to minimise the number of samples while preserving the variability of the data set. Specifically, a decision-making algorithm decides after each measurement made by the probe whether it should trigger a new sampling event. The mathematical formalism used in this section is constructed as follows: matrices are noted in bold with a capital letter (e.g. **X**), vectors are noted in bold with a lower case letter (e.g. **msv**), row and column indices are presented in lower case and italics (e.g. $_{i,j}$).

The Optimised Sampling Algorithm (OSA) is triggered after each measurement made by the mobile laboratory, *i.e.* every ten minutes. Like the ML automation, the OSA is written in python 3.7.6 , mainly based on the pandas 1.1.4 and numpy 1.18.3 packages (Harris et al. 2020; Reback et al. 2022). At each activation, the OSA takes as input 3 different datasets. Firstly, the measurements made by the ML since the beginning of the campaign. The corresponding data are collected in a data matrix **X** of dimension $n \times m$, with n the number of measurements made since the system was launched and m the number of parameters monitored (in this study, m = 7). Then, a second matrix **Xs** is defined, which groups together all the previous measurements that led to a sample being taken. This matrix **Xs** is of dimension $k \times m$ with k the number of samples. By construction, **Xs** $\subset$ **X** and $k < n$. Finally, the new measure for which the OSA must decide is noted **xnew** and corresponds to a vector of $1 \times m$ dimension.

This algorithm works in three main steps.

First, a pre-processing resulting in the standardisation of the **Xs** and **xnew** data (Eqn 1) is carried out:

$$\boldsymbol{X}_{i,j}^{\boldsymbol{std}} = \frac{\boldsymbol{X}_{i,j} - \boldsymbol{med}_{1,j}}{\boldsymbol{msv}_{1,j}} \qquad (Equation\ 1)$$

Calculation of $\mathbf{X}^{\mathbf{std}}$ is done element-wise on the ith-row j^{th}-column elements of **X**. **med** is a 1 x *m* vector containing the median of each parameter over the last 1008 rows of **X**, corresponding to the last week of data. The vector **msv**, of dimension 1 × *m*, represents the minimum significant variation used as a standard deviation. **msv** values are set by the user, considering the quality of the sensor signal, as well as the knowledge of the variability of the observations for the river. The pre-processing step is very important as it will impact the importance of each parameter in the decision process of sampling. For some parameters, such as pH, the noise level will be used to set the values in **msv** (*e.g.* the **msv** for pH has been chosen to be 0.2 even though a variation of 0.1 could be considered relevant for the environment). For others, the corresponding value of the **msv** can be increased so that there is no oversampling for every small variation of that parameter (*e.g.* the **msv** for conductivity was set to 25 µS cm^{-1} even though the noise is about 2 µS cm^{-1}). Following these recommendations, tests are performed to check if the msv vector is well balanced, *i.e.* variations of one parameter are not under considered compared to the others. Part D in the supplementary information presents examples of msv that are correct or in need of adjustment. If an unbalanced importance of a parameter is observed, **msv** can be readjusted by the user at any time during the process. Currently for this study, the **msv** vector is defined with the following values: 0.4 °C for temperature; 0.1 upH for pH; 25 µS/cm for conductivity; 5 FNU for turbidity; 0.5 mg/L for dissolved oxygen; 2 ppb for CDOM and 5 ppb for tryptophan.

Once standardised, the second step is to calculate the Euclidean distances between the new measurement **xnew** and the *k* samples available in **Xs** (Eqn 2).

$$\boldsymbol{d}_i = \sqrt{\sum_{j=1}^{7} \left(\mathbf{xnew}_j - \mathbf{Xs}_{i,j}\right)^2} \qquad (Equation\ 2)$$

where $\mathbf{d}_i$ is the distance between **xnew** and the *i-th* samples in **Xs.** The main idea behind the calculation of these distances is to determine whether the new measurement represents a new state of the system compared to previous samples. For this purpose, all distance value $\mathbf{d}_i$ are compared to a threshold value, denoted *t*. If one of these distances is smaller than *t*, it is considered that the measurement **xnew** is already represented in the **Xs** database. Conversely, if all distances are greater than *t*, this measurement is considered to represent a new state of the system. In this case, a sample is taken and **xnew** is added to the **Xs** database for the next ML measurements.

Thirdly, the threshold value *t* is calculated with the Equation 3:

$$t = dto \times a + b \qquad (Equation\ 3)$$

where slope *a* and intercept *b* values are chosen by the users, as explained in detail in the *Results & discussion* section. The coefficient *dto* is the distance between the origin and the new measurement, **xnew**. *dto* is defined as (Eqn 4):

$$dto = \sqrt{\sum_{j=1}^{7} \left(\mathbf{xnew}_j\right)^2} \qquad (Equation\ 4)$$

It should be noted that the parameters chosen for the calculation of *t* are of paramount importance to extract maximum information while balancing the number of samples collected. Making *t* dependent on the *dto* for each measurement tested by the OSA allows for a better adaptability to the variability of the system studied. In contrast to the proposed procedure, a fixed *t*-value could be chosen. However, this would make the sampling very sensitive to extreme events. Indeed, fixing a small value for t would allow to correctly detect fine and daily

variations. However, during extreme events, the mean value of *e.g* turbidity can be multiplied by 50 and, in this case, almost all measurements would lead to the decision of withdrawing a sample. Estimating t using Equation 4 allows overcoming this issue, translating into low threshold values for regular daily variations and higher values for extreme events. In this way, good sensitivity is ensured in normal conditions while oversampling is avoided during extreme events.

The overall functioning of the OSA is summarised in Figure 1.

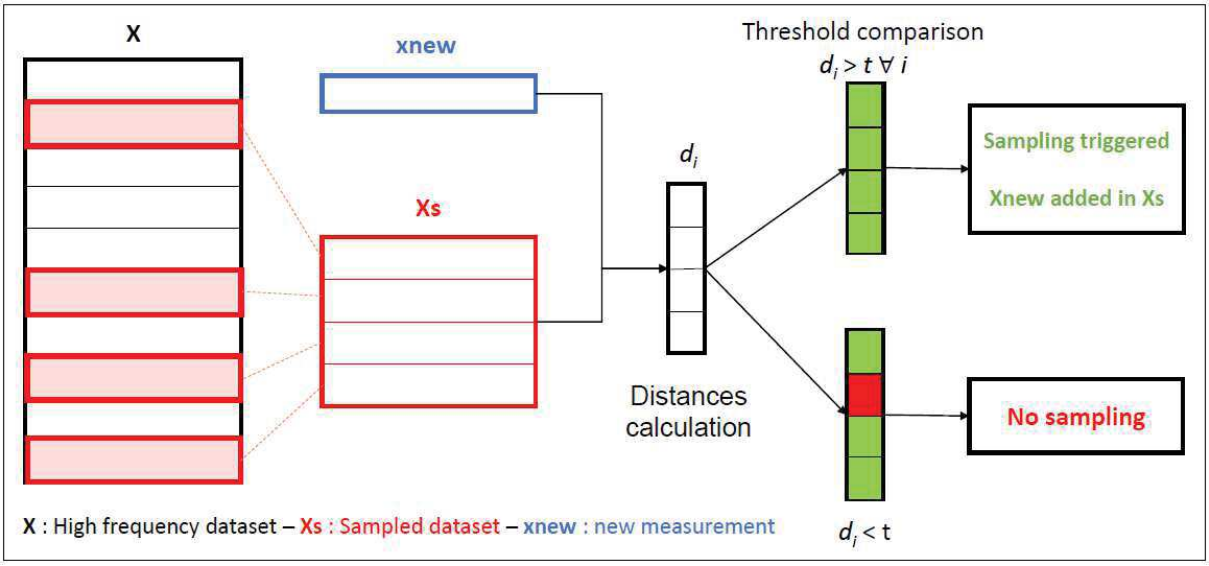

Figure 1: Schematic view of the OSA.

1.4.Performance control

Once the samples have been identified by the OSA, it is necessary to verify their relevance. A high frequency dataset (**Xrebuilt**, dimensions ($n \times m$)) is reconstructed from the sampled dataset (**Xs**). Each non-sampled point is assigned the parameter values of the closest sampled point. To estimate the adequacy of the relevance of samples, two approaches are taken. The first is calculating the Pearson correlation coefficient for each parameter measured by the

multiparameter probe. This evaluates the quality of the reconstruction of the complete dataset from the sampled point to a certain extent. The second is based on Principal Component Analysis (PCA). PCA is performed on both **Xrebuilt** and **X** and the loadings obtained are compared calculating Tucker Congruence Coefficient (Lorenzo-Seva and ten Berge 2006) between all principal components. In this way, we can assess the good conservation of high frequency data variability within the sampled dataset.

2. Results & discussion

2.1. Overview of the experimental dataset acquired

The first step in developing this algorithm (OSA) was to obtain a large dataset representative of the Marque River. For that purpose, a month's worth of data was collected using the multiparameter probe deployed in the ML. A total of 3754 measurements were performed from 23 March to 20 April 2021, representing 26 monitoring days, with a total loss of 2 measurement days (7.7 %) due to technical issues (Figure 2). Daily cycles of temperature, pH and dissolved oxygen are clearly evidenced due to the alternance of day and night times and the development of macrophytes during this period in this highly eutrophic river (Ivanovsky and al., 2016). During this monitoring, significant meteorological evolutions also took place: (i) air daily mean temperature values evolved strongly and ranged between 2.3°C on April 7th and 17.0°C on April 1st; and (ii) a heavy rainfall event was observed with 16.3 mm of water (10-11 April). The discharge of wastewaters from storm overflows was recorded during this event, leading to an important drop of dissolved oxygen and sharp peaks of dissolved organic matter. The input of rainwater in the river is also very significant as the conductivity dropped by around 40%. These events are very different (diel *vs*. punctual, small variations *vs*. plummeting/skyrocketing parameters) which makes this first dataset very relevant to optimize our algorithm.

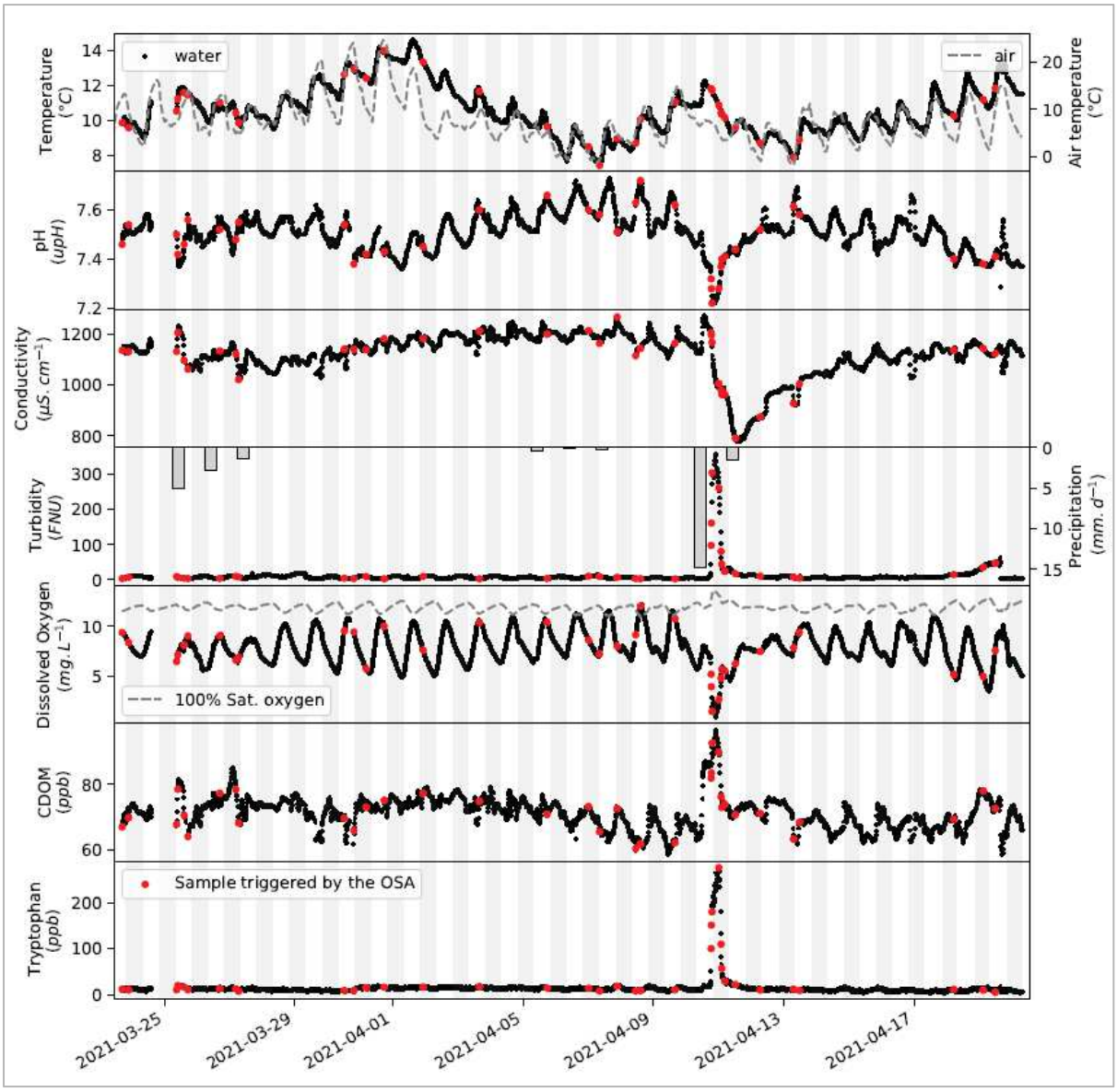

Figure 2: Set of data recorded by the multiprobe and used for OSA optimisation. The red dots represent the moments when the OSA triggers a sampling. Air temperature and daily pluviometry have been added for information.

2.2.Optimisation of the OSA

The behaviour and the associated performances of the OSA have been studied from the collected dataset. The first step is to define the best combinations of *a* and *b* used in the threshold value calculation. The way in which this value is calculated affects both the number of samples and their distribution. These choices were based on preliminary tests. Different samples sets are then generated, by testing combinations of *a* and *b* over a certain range (from 0.1 to 1 for a and from 0 to 6 for b, with steps of 0.1 and 0.5 respectively). For each samples set generated, the performance control is performed as described previously by calculating the correlation coefficient between **X** and **Xrebuilt** and by comparing the PCA.

To assess the performance quality of the sampling carried out by the OSA, it is also necessary to compare these results with other sampling methods. The first comparison is made against randomly selected samples (RandS) while the second comparison is performed with a fixed step sampling method (StepS). The average sampling rates are between 0.15 and 3 samples per day for each method. This is, in our case, an operationally feasible sampling frequency range for monitoring over several months while maintaining sensitivity to one-off and daily events.

The results of these different simulations are shown in Figure 3.

Logically, whatever the methods and correlations, increasing the sampling frequency improves the description of the dataset in a non-linear way. The first observable difference between the three methods is a better stability for the OSA of the correlations with the increase of the number of samples. The RandS and StepS methods indeed show strong disparities when increasing the frequencies.

Figure 3.A shows the evolution of the average Tucker Congruence Coefficient between principal components of **X** and **Xrebuilt**, calculated for the different methods. This coefficient

has the advantage of considering all the parameters under study. OSA consistently exhibits higher coefficients than the two other methods. Moreover, it is interesting to observe that a ceiling seems to be reached for frequencies of the order of 1 sample per day. The gain in this coefficient is then negligible for higher sampling frequencies.

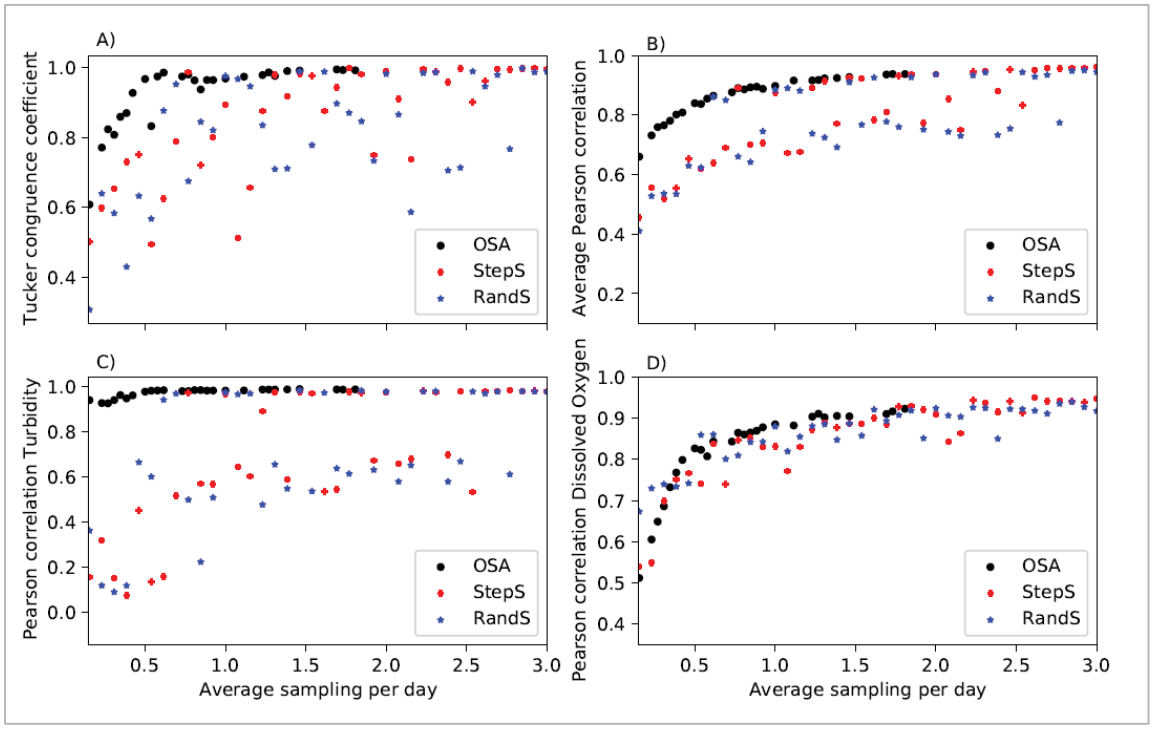

Figure 3: Comparison between the different sampling methods: OSA, fixed step (StepS) and random (RandS). For the OSA, each black dot represents a combination of a and b. Figure A shows the Tucker Congruence Coefficient. Figure B shows the average Pearson correlation. Figure C shows the Pearson correlation on turbidity. Figure D represents the Pearson correlation on Dissolved Oxygen.

Figure 3.B shows the mean value of the Pearson correlations between parameters in **X** and **Xrebuilt**. The use of the average of these coefficients allows to approximate a multivariate visualisation of the system. Again, the OSA shows both better results and greater stability compared to the other methods.

Figures 3.C and 3.D display the Pearson correlations of two parameters: turbidity and dissolved oxygen. These two correlations show very different behaviours for the OSA. For turbidity, the

OSA systematically gives a very high correlation where the other methods rarely manage to describe this signal correctly. The main reason is the variability of the turbidity signal (and equivalently the tryptophan). For both signals (see Figure 2), the measurements are quite stable except for a strong increase from 10 to 11 April caused by a heavy rainfall. This event has a strong impact on water quality for a very short time. For "classical" sampling methods, it is usually very difficult to take samples on this kind of short event. Conversely, the OSA makes possible in a systematic way, to consider this type of phenomenon whose impacts may be important and often poorly understood. The randomness of the ability of classical methods to sample these events is also reflected in the correlations with highly scattered values, resulting from the presence or absence of sampling during this stormy period.

For the dissolved oxygen (and comparably for temperature, pH, conductivity and CDOM), the behaviour of the OSA is quite different. For sampling frequencies between 0.5 and 2, OSA exhibits good results compared to other methods with high stability. For frequencies above 2, all three methods give comparable correlation values. However, for low frequencies (< 0.3 day^{-1}), the OSA indicates lower performance than the two other methods. This is due to the nature of the operation of the OSA and the dissolved oxygen signal. Indeed, as seen previously, the OSA systematically samples the rainfall event regardless of the sampling frequency, so that the few samples are mainly taken during this event. As a result, the dissolved oxygen values identified are not representative of the overall variability as shown in Figure 2. In other words, when only a few samples are taken, extreme events will be prioritized over small daily variations.

Finally, from these data, it is possible to choose a pair of values for the parameters a and b corresponding to the objectives and limitations of the study under consideration. Adjustments of the **msv** values can also be made to slightly adjust the sensitivity of the OSA on the different

parameters. However, these modifications must be made with an awareness of technical limitations and environmental variations.

2.3. Application of the OSA to a monitoring campaign

The OSA was used for a campaign conducted from April 20th to June 28th, 2021, on the Marque River. During this period, 103 samples were taken, corresponding to an average frequency of 1.6 samples per day. This frequency is higher than that predicted by the previous simulation (1.4), probably due to the high variability observed during the campaign and the strong weather changes due to the transition towards the summer season.

The OSA sampling system ensures a good representation of the environment, by taking samples during events that have a strong impact on the environment, regardless of their duration. Some examples of sampled events are shown Figure 4.

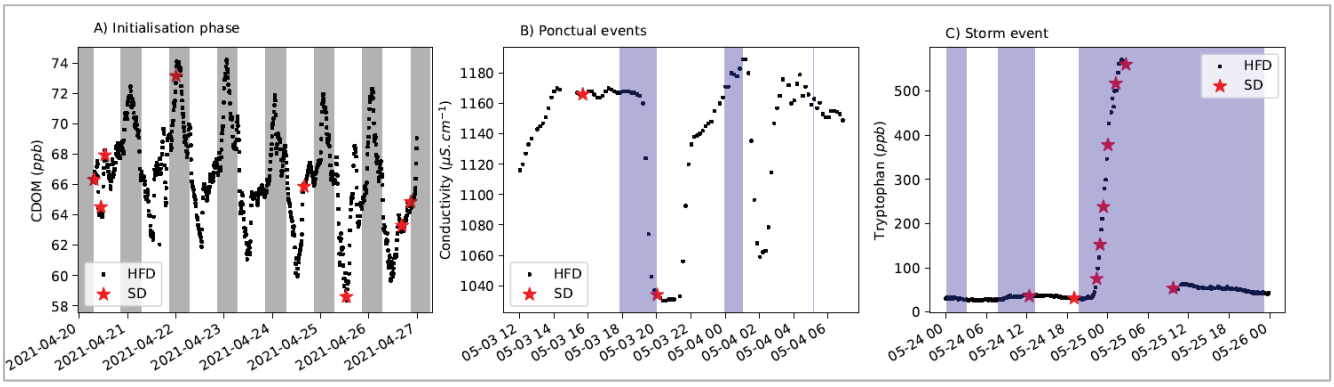

Figure 4: Three examples of the OSA response. Figure A shows the launch of the algorithm and its initialisation/discovery phase with day/night cycle in white/gray stripes. Figure B shows its reaction to a brief one-off phenomenon and its learning capacity. Figure C shows the ability of the algorithm to adapt its measurement frequency according to the observed variations. In B and C figures, the purple stripes correspond to the input of water from a nearby lake 500 m upstream of the station.

Figure 4.A. shows the launch of the OSA over the first 7 days, represented for only one parameter, with close sampling during the launch (initialization/discovery phase). This is

339 followed by periods without additional sampling as variability remains as low as previously.
340 Figure 4.B. shows a one-off event of high dilution of the river by the overflow of the retention
341 basin (the Heron lake), located just upstream. The purple areas correspond to the periods during
342 which the water from this pond is pumped into the river; the time lag between the discharge
343 and the impact on the conductivity is due to the distance between the discharge and the mobile
344 laboratory. The OSA can trigger a sampling during this brief period (less than two hours), but
345 also not to take a sample again when this event reappears some hours later. The last example
346 (Figure 4.C.) shows the ability of the OSA to multiply samples during periods of high
347 variability, here using the example of heavy rainfall leading to a large increase in turbidity.
348 These periods are often critical for environmental studies and require special attention, here
349 represented by the increase in the number of samples taken over a short period.

350 The parameters *a* and *b* identified in the test phase produced excellent results in this campaign.
351 All correlation coefficients are above 0.96, with a Tucker congruence of 0.998. These excellent
352 results despite different environmental changes than those observed during the simulation
353 clearly validate the transposition of the OSA settings over different periods (HF data and the
354 sampling points are displayed in the *Supplementary Information*, as well as the performance
355 indicator on this period).

356

357 **2.4. OSA limitation**

358 According to these findings and our experience feedback in the field, several points of vigilance
359 must be mentioned for an optimized deployment in routine of the OSA.

360 As for any data treatment, bad data lead to bad analysis. The OSA is optimised to detect changes
361 and will be especially sensitive to probe fouling and drift as well as recalibrations and cleaning
362 of the instrument. For example, pH sensor re-calibration after a long period without

maintenance (*e.g.* several weeks) led to an over-sampling of the daily cycles, despite them having been characterized previously. To limit this kind of bias, a regular maintenance of the multiprobe have been implemented (cleaning and calibration). A weekly frequency has been chosen in this river based on the observation of the fouling, but it could be adapted depending on the characteristics of the studied water body and weather conditions (*e.g.* summer *vs*. winter). Furthermore, traceability of the maintenance and calibration must be ensured, if possible automatically, to allow an *a posteriori* understanding of the sampling by the OSA.

OSA is also intended to be a tool for detecting the variability occurring in a system. With good optimisation, it should be able to sample during both small and extreme phenomena. However, for lower sampling frequencies (of the order of a week, for example), only extreme events will be sampled by the OSA. The "baseline" status of the river will systematically be dismissed by the algorithm and so the information associated with it as well. Figure 3.D confirms that a misrepresentation can be observed at low sampling rate and that the OSA can become worst that random sampling in such configuration.

The seven parameters measured with the probe can sometimes be much correlated (*e.g.* dissolved oxygen with pH are correlated with an R=0.79 over 9 months in 2021). Therefore, there is a risk that using them all can give a lot of statistical importance to the group of parameters varying together. However, there is always the chance that a decorrelation might occur, indicative of a new phenomenon happening, and the OSA should in this case be able to detect it. That is why the choice was made to keep all parameters.

Finally, with a more operational vision, the non-regular distribution of samples over time can be problematic. Indeed, it is possible to have no samples over several days and then 8 samples over one day during a storm. It requires flexible human resources and alert systems to grab collected samples.

Conclusion

This study was dedicated to the development, optimisation, and validation of a decision support algorithm for taking samples following multiparametric HF measurements. It allows the overall variability of the data to be maintained while reducing the number of samples collected. OSA is particularly suitable for sampling short-lived events with a high environmental impact.

To our best knowledge, this is the first approach of this type of sampling based on on-line multiparameter measurements. This tool is a particular response to the difficulty observed in many studies of taking samples on short and difficult to predict events. Even if it remains a perfectible tool (e.g. **msv** values could be further optimised in the future), the realisation of a campaign in spring 2021 has proved its operational applicability.

This type of sampling will be very useful for studies where a large variety of samples are necessary to insure a statistical robustness. Typically, it will be interesting for dissolved organic matter studies in which fluorescence excitation emission matrices are measured, as the exploitation of these matrices with the deconvolution algorithm Parafac requires some variability in the dataset to have a robust model in the end. More generally, OSA could be of interest in any environmental study that could benefit from such a system as it should improve the strength of the correlation or PCA results.

Acknowledgment

We acknowledge Artois-Picardie Water Agency (AEAP) and the region Haute de France for cofunding the PhD of JM. The Region Hauts de France and the French Government are also warmly acknowledged through the founding of the CPERs Climibio and ECRIN that funded part of the monitoring station. We are grateful to Sourceo for allowing us to deploy the station on their site and to the Lille European Metropolis (MEL) for providing complementary

information and WWTP data. The authors wish to thank the European Commission funding for the LIFE RUBIES project (LIFE20 ENV/000179). We thank the lab members Jean-Pierre Verwaerde, Viviane Blotiau and Vincent Carlucci for their help with building and maintaining the station.

References:

Aguilera, R., Livingstone, D.M., Marcé, R., Jennings, E., Piera, J., Adrian, R., 2016. Using dynamic factor analysis to show how sampling resolution and data gaps affect the recognition of patterns in limnological time series. *Inland Waters* **6**, 284–294. https://doi.org/10.1080/IW-6.3.948

Bieroza, M.Z., Heathwaite, A.L., 2016. Unravelling organic matter and nutrient biogeochemistry in groundwater-fed rivers under baseflow conditions: Uncertainty in in situ high-frequency analysis. *Science of The Total Environment* **572**, 1520–1533. https://doi.org/10.1016/j.scitotenv.2016.02.046

Bieroza, M.Z., Heathwaite, A.L., 2015. Seasonal variation in phosphorus concentration–discharge hysteresis inferred from high-frequency in situ monitoring. *Journal of Hydrology* **524**, 333–347. https://doi.org/10.1016/j.jhydrol.2015.02.036

Carstea, E.M., Baker, A., Bieroza, M., Reynolds, D., 2010. Continuous fluorescence excitation–emission matrix monitoring of river organic matter. *Water Research* **44**, 5356–5366. https://doi.org/10.1016/j.watres.2010.06.036

Ferrant, S., Laplanche, C., Durbe, G., Probst, A., Dugast, P., Durand, P., Sanchez-Perez, J.M., Probst, J.L., 2013. Continuous measurement of nitrate concentration in a highly event-responsive agricultural catchment in south-west of France: is the gain of information useful?: HIGH-FREQUENCY SAMPLING OF NITRATE FLUSHING. *Hydrol. Process.* **27**, 1751–1763. https://doi.org/10.1002/hyp.9324

Gunatilaka, A., Diehl, P., 2001. A Brief Review of Chemical and Biological Continuous Monitoring of Rivers in Europe and Asia. In 'Biomonitors and Biomarkers as Indicators of Environmental Change 2' (Eds. Butterworth, F.M., Gunatilaka, A., Gonsebatt, M.E.). Springer US, Boston, MA, pp. 9–28. https://doi.org/10.1007/978-1-4615-1305-6_2

Halliday, S., Skeffington, R., Bowes, M., Gozzard, E., Newman, J., Loewenthal, M., Palmer-Felgate, E., Jarvie, H., Wade, A., 2014. The Water Quality of the River Enborne, UK: Observations from High-Frequency Monitoring in a Rural, Lowland River System. *Water* **6**, 150–180. https://doi.org/10.3390/w6010150

Harris, C.R., Millman, K.J., van der Walt, S.J., Gommers, R., Virtanen, P., Cournapeau, D., Wieser, E., Taylor, J., Berg, S., Smith, N.J., Kern, R., Picus, M., Hoyer, S., van Kerkwijk, M.H., Brett, M., Haldane, A., del Río, J.F., Wiebe, M., Peterson, P., Gérard-Marchant, P., Sheppard, K., Reddy, T., Weckesser, W., Abbasi, H., Gohlke, C., Oliphant, T.E., 2020. Array programming with NumPy. *Nature* **585**, 357–362. https://doi.org/10.1038/s41586-020-2649-2

Ivanovsky, A., Criquet, J., Dumoulin, D., Alary, C., Prygiel, J., Duponchel, L., Billon, G., 2016. Water quality assessment of a small peri-urban river using low and high frequency monitoring. *Environ. Sci.: Processes Impacts* **18**, 624–637. https://doi.org/10.1039/C5EM00659G

Jarvie, H.P., Sharpley, A.N., Kresse, T., Hays, P.D., Williams, R.J., King, S.M., Berry, L.G., 2018. Coupling High-Frequency Stream Metabolism and Nutrient Monitoring to Explore Biogeochemical Controls on Downstream Nitrate Delivery. *Environ. Sci. Technol.* **52**, 13708–13717. https://doi.org/10.1021/acs.est.8b03074

Khamis, K., Bradley, C., Hannah, D.M., 2020. High frequency fluorescence monitoring reveals new insights into organic matter dynamics of an urban river, Birmingham, UK. *Science of The Total Environment* **710**, 135668. https://doi.org/10.1016/j.scitotenv.2019.135668

Lewis, J., Eads, R., 2009. Implementation guide for turbidity threshold sampling: principles, procedures, and analysis (No. PSW-GTR-212). U.S. Department of Agriculture, Forest Service, Pacific Southwest Research Station, Albany, CA. https://doi.org/10.2737/PSW-GTR-212

Liu, X., Beusen, A.H.W., Van Beek, L.P.H., Mogollón, J.M., Ran, X., Bouwman, A.F., 2018. Exploring spatiotemporal changes of the Yangtze River (Changjiang) nitrogen and phosphorus sources, retention and export to the East China Sea and Yellow Sea. *Water Research* **142**, 246–255. https://doi.org/10.1016/j.watres.2018.06.006

Lorenzo-Seva, U., ten Berge, J.M.F., 2006. Tucker's Congruence Coefficient as a Meaningful Index of Factor Similarity. *Methodology* **2**, 57–64. https://doi.org/10.1027/1614-2241.2.2.57

Marcé, R., George, G., Buscarinu, P., Deidda, M., Dunalska, J., de Eyto, E., Flaim, G., Grossart, H.-P., Istvanovics, V., Lenhardt, M., Moreno-Ostos, E., Obrador, B., Ostrovsky, I., Pierson, D.C., Potužák, J., Poikane, S., Rinke, K., Rodríguez-Mozaz, S., Staehr, P.A., Šumberová, K., Waajen, G., Weyhenmeyer, G.A., Weathers, K.C., Zion, M., Ibelings, B.W., Jennings, E., 2016. Automatic High Frequency Monitoring for Improved Lake and Reservoir Management. *Environ. Sci. Technol.* **50**, 10780–10794. https://doi.org/10.1021/acs.est.6b01604

Meyer, A.M., Fuenfrocken, E., Kautenburger, R., Cairault, A., Beck, H.P., 2021. Detecting pollutant sources and pathways: High-frequency automated online monitoring in a small rural French/German transborder catchment. *Journal of Environmental Management* **290**, 112619. https://doi.org/10.1016/j.jenvman.2021.112619

Nimick, D.A., Gammons, C.H., Parker, S.R., 2011. Diel biogeochemical processes and their effect on the aqueous chemistry of streams: A review. *Chemical Geology* **283**, 3–17. https://doi.org/10.1016/j.chemgeo.2010.08.017

Piniewski, M., Marcinkowski, P., Koskiaho, J., Tattari, S., 2019. The effect of sampling frequency and strategy on water quality modelling driven by high-frequency monitoring data in a boreal catchment. *Journal of Hydrology* **579**, 124186. https://doi.org/10.1016/j.jhydrol.2019.124186

Reback, J., Jbrockmendel, McKinney, W., Van Den Bossche, J., Augspurger, T., Roeschke, M., Hawkins, S., Cloud, P., Gfyoung, Sinhrks, Hoefler, P., Klein, A., Terji Petersen, Tratner, J., She, C., Ayd, W., Naveh, S., JHM Darbyshire, Garcia, M., Shadrach, R., Schendel, J., Hayden, A., Saxton, D., Gorelli, M.E., Fangchen Li, Zeitlin, M., Jancauskas, V., McMaster, A., Wörtwein, T., Battiston, P., 2022. pandas-dev/pandas: Pandas 1.4.2. Zenodo. https://doi.org/10.5281/ZENODO.3509134

Reynolds, K.N., Loecke, T.D., Burgin, A.J., Davis, C.A., Riveros-Iregui, D., Thomas, S.A., St. Clair, M.A., Ward, A.S., 2016. Optimizing Sampling Strategies for Riverine Nitrate Using High-Frequency Data in Agricultural Watersheds. *Environ. Sci. Technol.* **50**, 6406–6414. https://doi.org/10.1021/acs.est.5b05423

Rode, M., Wade, A.J., Cohen, M.J., Hensley, R.T., Bowes, M.J., Kirchner, J.W., Arhonditsis, G.B., Jordan, P., Kronvang, B., Halliday, S.J., Skeffington, R.A., Rozemeijer, J.C., Aubert, A.H., Rinke, K., Jomaa, S., 2016. Sensors in the Stream: The High-Frequency Wave of the Present. *Environ. Sci. Technol.* **50**, 10297–10307. https://doi.org/10.1021/acs.est.6b02155

Searcy, R.T., Boehm, A.B., 2021. A Day at the Beach: Enabling Coastal Water Quality Prediction with High-Frequency Sampling and Data-Driven Models. *Environ. Sci. Technol.* **55**, 1908–1918. https://doi.org/10.1021/acs.est.0c06742

Seifert, A.-G., Roth, V.-N., Dittmar, T., Gleixner, G., Breuer, L., Houska, T., Marxsen, J., 2016. Comparing molecular composition of dissolved organic matter in soil and stream water: Influence of land use and chemical characteristics. *Science of The Total Environment* **571**, 142–152. https://doi.org/10.1016/j.scitotenv.2016.07.033

Seifert-Dähnn, I., Furuseth, I.S., Vondolia, G.K., Gal, G., de Eyto, E., Jennings, E., Pierson, D., 2021. Costs and benefits of automated high-frequency environmental monitoring – The case of lake water

management. *Journal of Environmental Management* **285**, 112108. https://doi.org/10.1016/j.jenvman.2021.112108

Shultz, M., Pellerin, B., Aiken, G., Martin, J., Raymond, P., 2018. High Frequency Data Exposes Nonlinear Seasonal Controls on Dissolved Organic Matter in a Large Watershed. *Environ. Sci. Technol.* **52**, 5644–5652. https://doi.org/10.1021/acs.est.7b04579

Superville, P.-J., Prygiel, E., Magnier, A., Lesven, L., Gao, Y., Baeyens, W., Ouddane, B., Dumoulin, D., Billon, G., 2014. Daily variations of Zn and Pb concentrations in the Deûle River in relation to the resuspension of heavily polluted sediments. *Science of The Total Environment* **470–471**, 600–607. https://doi.org/10.1016/j.scitotenv.2013.10.015

Vaughan, M.C.H., Bowden, W.B., Shanley, J.B., Vermilyea, A., Schroth, A.W., 2019. Shining light on the storm: in-stream optics reveal hysteresis of dissolved organic matter character. *Biogeochemistry* **143**, 275–291. https://doi.org/10.1007/s10533-019-00561-w

Optimising punctual water sampling with an on-the-fly algorithm based on multiparameter high-frequency measurements

Supplementary information

Jérémy Mougin[1], Pierre-Jean Superville[1], Cyril Ruckebusch[1], Gabriel Billon[1]*

[1]Université Lille, CNRS, UMR 8516 - LASIRE, LAboratoire de Spectroscopie pour les Interactions, la Réactivité et l'Environnement, F-59000 Lille, France.

Content

A. Map of the site

The monitoring station is situated in Villeneuve d'Ascq, near Lille, in northern France, on the Marque River. Both rural and urban pressures impact this small river. Specifically on the site of the monitoring, 3 inputs can be highlighted:

- the wastewater treatment plant of Villeneuve d'Ascq (150 000 inhabitant equivalent) 3km upstream.
- the Heron Lake. Its waters are a mix of rainwater and some domestic untreated waters, biologically treated in a chain of lakes ending in the Heron Lake. When the level of the Lake is too high, the water is pumped into the Marque River.
- The Petite Marque is a network of ditches in the middle of fields with a few occasional farms. Agricultural and domestic impacts can be expected.

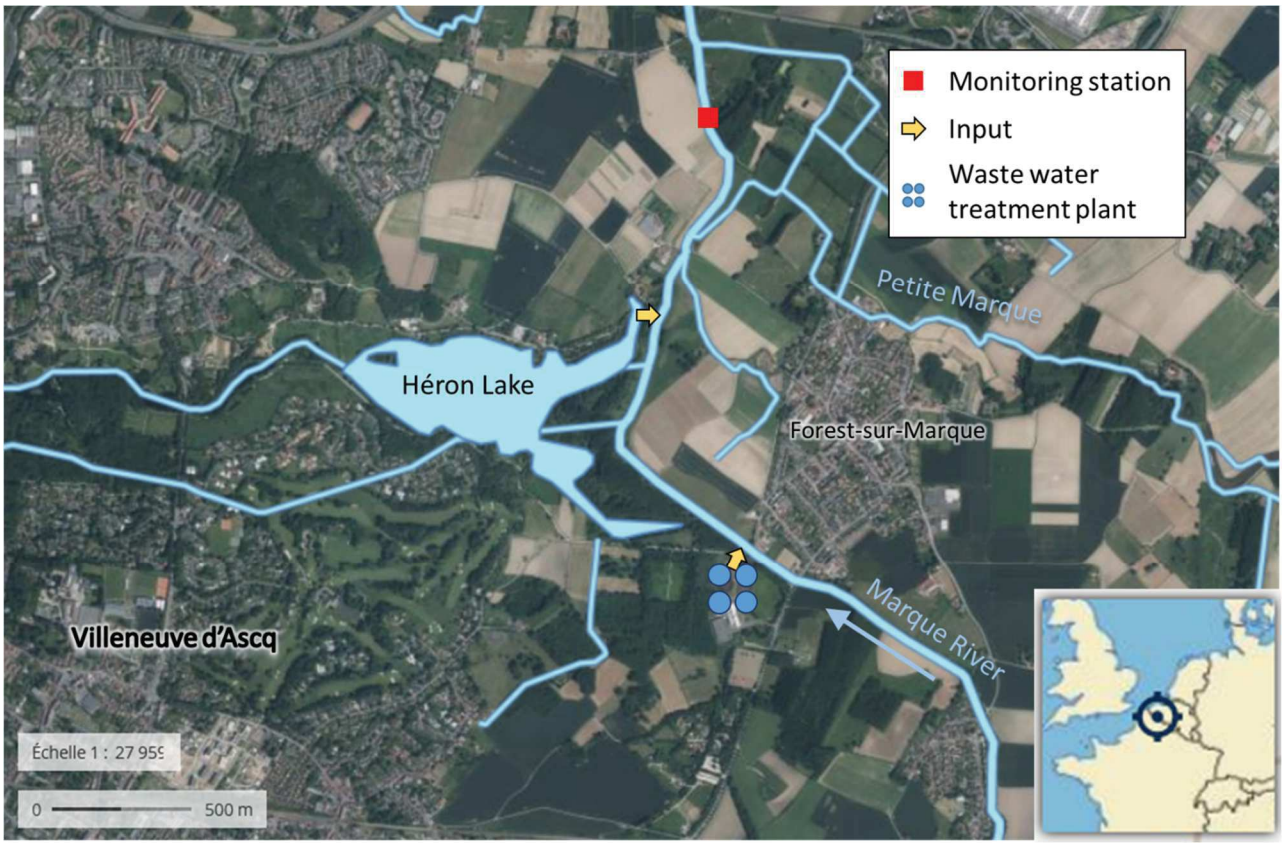

B. First campaign results

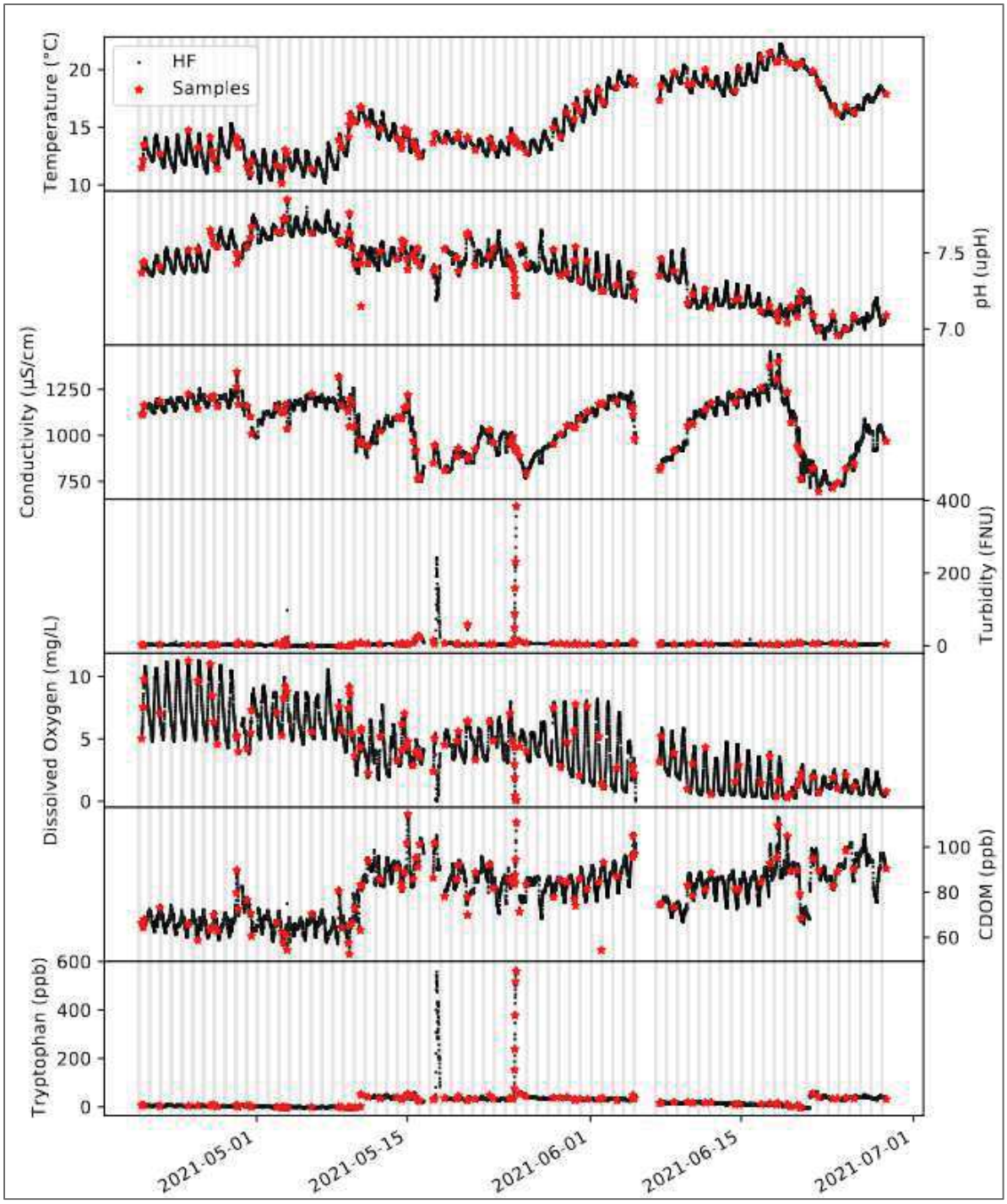

It can be noted that the first big storm was not sampled due to a clogging of the automated sampler.

C. OSA performance during the campaign

Parameter correlation between the original high frequency dataset and the dataset rebuilt from the samples:

	Temperature	pH	Conductivity	Turbidity	Dissolved O_2	CDOM	Tryptophane
Parameter self-correlation	0.98	0.99	0.97	0.98	0.97	0.96	0.99

PCA self-correlation, i.e. Tucker congruence coefficient between the original high frequency dataset and the dataset rebuilt from the samples:

	PC1 rebuilt (47 %)	PC2 rebuilt (26 %)	PC3 rebuilt (13 %)	PC4 rebuilt (6 %)	PC5 rebuilt (4 %)	PC6 rebuilt (2 %)	PC7 rebuilt (1 %)
PC1 original (48 %)	**0.999**	0.039	0.012	0.002	0.001	0.001	0.011
PC2 original (26 %)	-0.039	**0.997**	-0.055	0.018	-0.027	0.004	0.001
PC3 original (13 %)	-0.014	0.055	**0.997**	-0.038	-0.005	-0.009	0.011
PC4 original (6 %)	0.001	0.016	-0.039	**0.997**	0.008	-0.060	-0.011
PC5 original (4 %)	0.002	-0.027	-0.004	-0.008	**-0.999**	-0.004	-0.003
PC6 original (2 %)	-0.001	-0.003	0.006	-0.061	-0.004	**0.996**	0.051
PC7 original (1 %)	-0.011	-0.002	0.012	-0.008	-0.003	-0.051	**0.998**

D. Checking and optimizing the *msv*

The figure D.1 presents the Pearson correlation coefficient between the raw data and the rebuilt data for different ways of sampling. It shows in particular the importance of choosing properly the values of the minimal significant variation, *msv.*

The black points in the Figure D.1 correspond to the chosen *msv* for the rest of the study. The values for each parameter can be found in the Table D.2. in the line *msv* OSA. It can be seen that most of the Pearson correlation coefficient are quite good. The lowest is for pH (R=0.79) but this parameter is very noisy so it is not expected to have a perfect correlation.

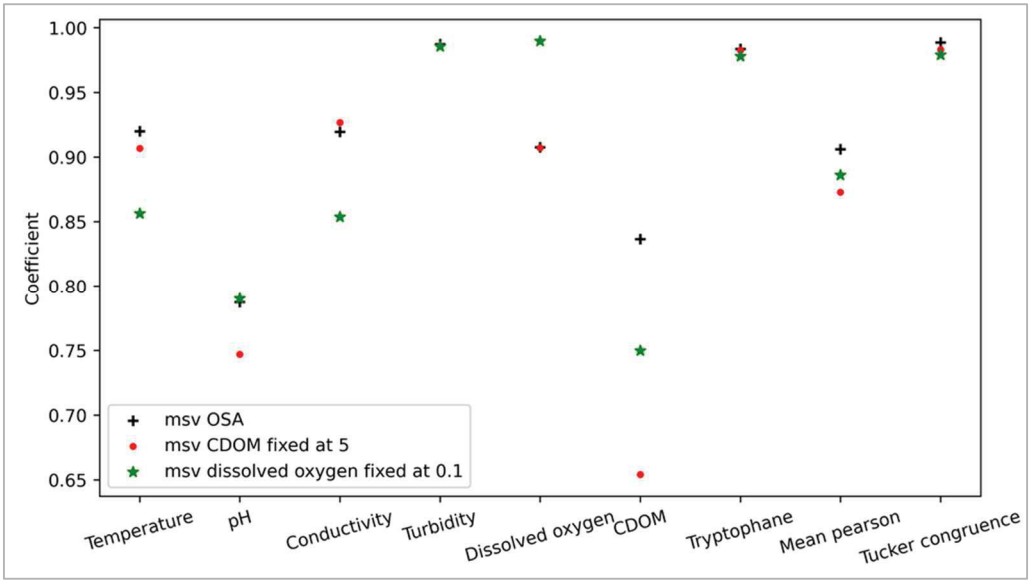

Figure D.1: Pearson correlation coefficient between the raw data and the rebuilt data for different values of *msv*.

Table D.2: values of the msv for the seven parameters

	Temp.	pH	Cond.	Turb.	Diss. O_2	CDOM	Trypt.
msv OSA	0.4	0.1	25	5	**0.5**	**2**	5
msv 2 CDOM = 5	0.4	0.1	25	5	0.5	**5**	5
msv 3 DO = 0.1	0.4	0.1	25	5	**0.1**	2	5

If the *msv* for a parameter is increased, *e.g.* CDOM msv is changed from 2 to 5, a lower sensitivity toward this parameter should be expected. And a decrease in the correlation coefficient is indeed observed, from R=0.84 to R=0.65.

If the *msv* for a parameter is decreased, *e.g*. Dissolved oxygen *msv* is changed from 0.5 to 0.1, smaller variation of oxygen concentration will be detected as significant. Representativity of our samples are now increase in term of oxygen (R goes from 0.91 to 0.99). But it is important to note that over-weighing dissolved oxygen has consequences on other parameters. Temperature (R= 0.92 to 0.86), conductivity (0.91 to 0.85) and CDOM (0.84 to 0.75) have a lower correlation coefficient, indicating a worst representativity of the sample. In a way, most of the samples are now dedicated to improve the O_2 signal and less are left for the other parameters. Therefore it is important to have a test phase in order to properly balance this *msv* vector.